

Dissipative superconductivity: a universal non-equilibrium state of nanowires

Yu Chen^{1,2}, Yen-Hsiang Lin^{2,4}, Stephen Snyder^{2,5}, Allen Goldman², and Alex Kamenev^{2,3}

¹*Department of Physics, University of California - Santa Barbara, Santa Barbara, CA 93106, USA*

²*School of Physics and Astronomy, University of Minnesota, Minneapolis, MN 55455, USA*

³*William I. Fine Theoretical Physics Institute, University of Minnesota, Minneapolis, MN 55455, USA*

⁴*Department of Physics, University of Michigan, Ann Arbor, MI, 48109 and*

⁵*Intel Corp., Portland OR, 97124*

(Dated: October 21, 2021)

The ability to carry electric current with zero dissipation is the hallmark of superconductivity.[1] It is this very property which is used in applications from MRI machines to LHC magnets. But, is it indeed the case that superconducting order is incompatible with dissipation? One notable exception, known as vortex flow, takes place in high magnetic fields.[2] Here we report observation of dissipative superconductivity in far more basic configurations: superconducting nanowires with superconducting leads. We provide evidence that in such systems, normal current may flow in the presence of superconducting order throughout the wire. The phenomenon is attributed to the formation of a non-equilibrium state, where superconductivity coexists with dissipation, mediated by the so-called Andreev quasiparticles. Besides promise for applications such as single-photon detectors,[3] the effect is a vivid example of a controllable non-equilibrium state of a quantum liquid. Thus our findings provide an accessible generic platform to investigate conceptual problems of out-of-equilibrium quantum systems.

With applications ranging from infrared detectors[4] to prototypical qubits[5, 6], superconducting nanocircuitry has emerged in recent years as a fascinating area of research. Its fundamental significance lies in *e.g.* phase-sensitive studies of pairing mechanisms in novel superconductors[7, 8] and access to a wealth of non-equilibrium quantum phenomena.[9] A key element of such circuitry - superconducting nanowires, are known to be susceptible to strong fluctuations. Their most spectacular manifestations are phase slips (PSs) of the superconducting order parameter, which lead to dissipation within a nominally dissipationless superconducting state.[10–12] Observing and studying such dissipative superconductivity has turned out to be a challenge. The culprits are non-equilibrium quasiparticles massively generated by PSs. If not removed efficiently, they tend to overheat the nanowire, driving it into the normal state. For example, thin MoGe[13, 14] and Al wires[15, 16] appear to be switched into the normal state by a single PS. The return to the superconducting state requires a signif-

icant decrease of the drive current, leading to hysteretic I-V characteristics.

In experiments reported here we overcome the excess heating by an improved fabrication process (see Methods for details). Electrically transparent interfaces between the wire and the leads allow for a fast escape of non-equilibrium quasiparticles into the environment. By choosing Zn as the growth material,[17] we are able to fabricate quasi-1D wires whose length L is significantly shorter than the inelastic relaxation length L_{in} , yet much longer than the coherence length $\xi \approx 250\text{nm}$. These bring us to a situation in which quasiparticles form a peculiar non-equilibrium distribution, governed by Andreev reflections from the boundaries with the superconducting leads. As a result, we observe a non-hysteretic dissipative state, which still exhibits distinct superconducting features such as a supercurrent and a sensitivity to weak magnetic fields.

In Fig. 1a, we show I-V characteristics of sample A, measured at temperatures from 50 to 750 mK in a well-filtered dilution refrigerator 1 (see Methods for details). Over a range of currents, flanked by the bottom and top threshold values $I_b < I < I_t$, the voltage across the nanowire exhibits a nearly flat plateau at $V_0 = 52.5 \pm 1.2 \mu\text{V}$ (for $T \lesssim 450$ mK). This indicates a peculiar dissipative state, which is distinctly different from the normal state. It is important to note that both I_t and I_b are factor of $30 \sim 50$ smaller than the estimated depairing critical current of the wire.[18] Collecting I_b and I_t together with I_c , where the system turns normal, we construct a temperature – current phase diagram, shown in Fig. 1b. It shows that as the temperature increases, the voltage plateau is compressed and eventually disappears at about 650 mK. This temperature dependence resembles that of the superconducting order parameter, suggesting that the dissipative voltage plateau state is associated with the superconducting order.

Performing measurements on different devices, we found a remarkable universality associated with the voltage plateau. In Fig. 1c-f, we compare the I-V characteristics of sample A with two other Zn samples B and C as well as an Al sample D, all measured at 450 mK. These samples differ from sample A both in their geometry and normal state resistance, and were measured in a different weakly-filtered refrigerator 2. Despite some

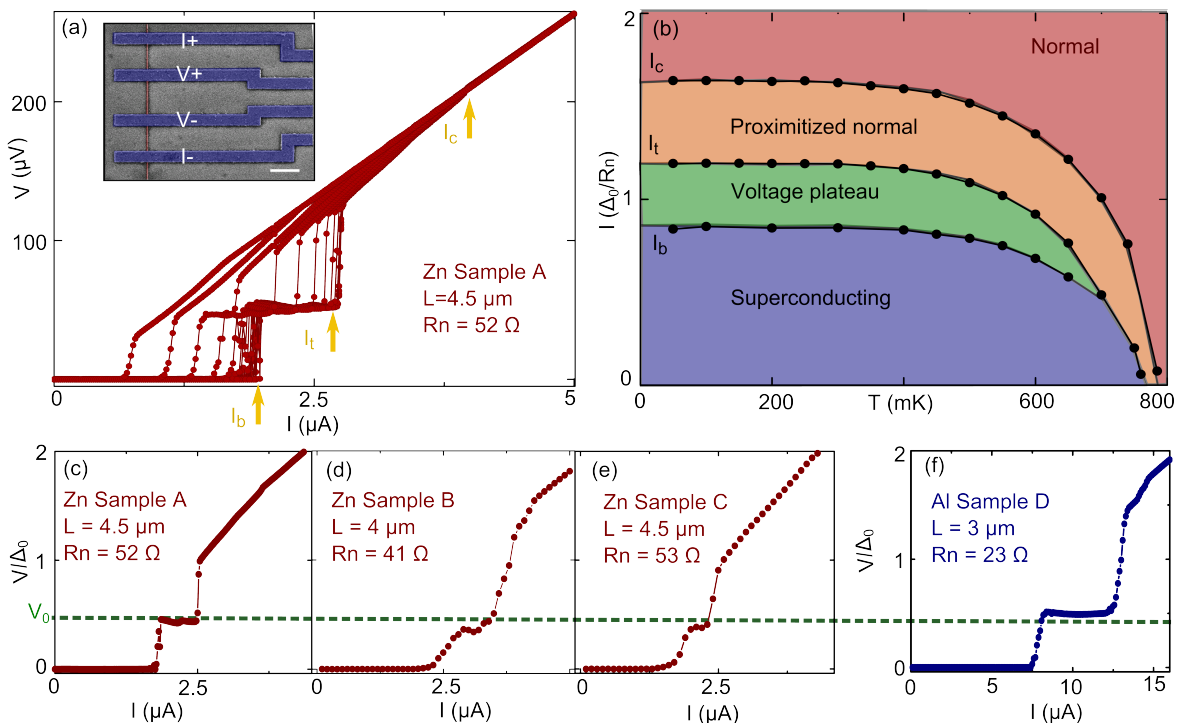


Figure 1. **Experimental observation of the voltage plateau.** a) The I-V characteristics of sample A, at temperatures from 50 mK to 750 mK (right to left) with a 50 mK interval. The voltage plateau with $V_0 \sim 52 \mu\text{V}$ is visible between the bottom and top threshold currents I_b and I_t . The scale bar represents $2 \mu\text{m}$. b) The temperature – current phase diagram, showing the voltage plateau existing at $T \lesssim 650$ mK. c-f) The I-V characteristics of Zn sample A-C and Al sample D, measured at 450 mK. Sample A was measured in the well-filtered cryostat 1, while samples B-D – in the weakly-filtered cryostat 2. The voltage axes are scaled to the BCS energy gap $2\Delta_0 = 3.52T_c$ for each sample. The voltage plateau of all samples collapses onto $V_0/\Delta_0 \sim 0.43 \pm 0.05$, providing the evidence for the universality of the plateau state.

smearing by unfiltered noise, the plateau voltage V_0 remains nearly unchanged for all of the Zn wires. The only exception is Al sample D, with the voltage plateau at $V_0 \simeq 93.2 \pm 1.3 \mu\text{V}$. Rescaling this voltage with the BCS superconducting gap $2\Delta_0 \approx 3.52T_c$, we found that the plateaus in all samples fall close to the same universal line $eV_0/\Delta_0 = 0.43 \pm 0.05$ (the ratio for all samples is listed in Supplemental Material [19]).

Another remarkable feature of the voltage plateau state is its onset through a region of stochastic bistability. It is revealed by time-domain measurements, with the voltage measured with a repetition rate of 3 Hz under a sustained constant current. In Fig. 2a we show a time trace of the measured voltage at $I = 1.95 \mu\text{A}$ and $T = 50\text{mK}$. The system exhibits random switchings between the superconducting and voltage plateau states with a characteristic time scale of a few seconds, indicating an intrinsic bistability. To quantify stability of the two competing states we define lifetimes: τ_{sc} and τ_{vp} as the averaged residence times in the superconducting and the voltage plateau states respectively. Figure 2b shows their dependencies on the applied current throughout the transition range. Increasing the current, leads to

an exponential growth of the voltage plateau lifetime τ_{vp} and the reduction of the superconducting lifetime τ_{sc} , albeit at a smaller rate. It is worth mentioning that the two lifetimes are nearly temperature independent until $T \sim 400$ mK, above which τ_{vp} increases and τ_{sc} decreases exponentially.[19]

The observed dissipative state exhibits counterintuitive magnetic field dependence. One could expect that the magnetic field suppresses superconductivity, thus decreasing τ_{sc} and possibly increasing τ_{vs} . In fact, the exact opposite happens. As shown in Fig. 2c, a magnetic field of merely a few G stabilizes the superconducting state, *increasing* its lifetime by more than an order of magnitude, simultaneously decreasing the voltage plateau lifetime by two orders of magnitude. This behavior is consistently observed through the entire transition range of currents.

The *enhancement* of superconductivity by magnetic field is even more apparent by inspecting I-V characteristics at different fields, Fig. 2d. It is evident that the field shifts the bottom critical current I_b to higher values, stabilizing the superconducting state. Such a stabilization is in fact a result of the suppression of the

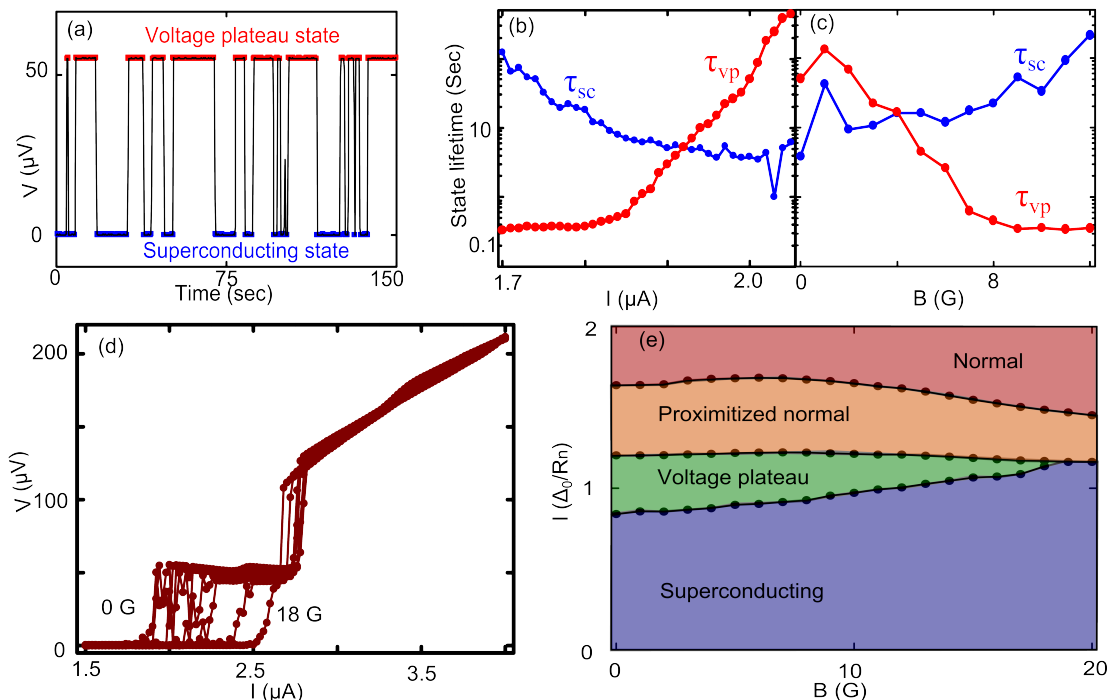


Figure 2. **The onset through bistability and the magnetic response of the voltage plateau.** a) The real-time evolution of the voltage, for sample A hold at a fixed current of $1.95 \mu A$ and at 50 mK. The system undergoes stochastic switching between the superconducting and the voltage plateau states. b) The average lifetime of the superconducting, τ_{sc} , and the voltage plateau, τ_{vp} states, at elevated currents. The transition is accomplished by suppressing the superconducting state and stabilizing the voltage plateau state. c) The average lifetimes as functions of perpendicular magnetic field. A magnetic field of only few G suppresses the lifetime of the voltage plateau state over two orders of magnitude. d) The I-V characteristics at magnetic fields from 0 to 18 G, with a 2 G interval. The bottom critical current I_b is seen to increase from $\sim 1.8 \mu A$ to $\sim 2.5 \mu A$. e) Magnetic field – current phase diagram shows the high sensitivity of the voltage plateau to magnetic field. The plateau disappears at 19 G.

voltage plateau state. This is best seen in the critical current vs. magnetic field phase diagram, Fig. 2e. The range of currents supporting the voltage plateau decreases rapidly from below until the plateau collapses at 19 G. Correspondingly the phase space of the superconducting state expands. We thus observe a rather counter-intuitive non-equilibrium phenomenon: keeping the current within the voltage plateau regime and *increasing* the magnetic field, brings the system from the dissipative *into* the superconducting state. This is consistent with the reported *magnetic-field-induced superconductivity* and *anti-proximity effect*. [20–23] It is now apparent that the magnetic field induced superconductivity originates with the collapse of the voltage plateau state, providing an intriguing connection between the two effects.

It is crucial to distinguish the observed voltage plateau state from other phenomena. It is different from phase slip centers, seen in long superconducting whiskers and characterized by a constant differential resistance, [18, 24] as opposed to a constant voltage. The plateau can't be a giant Shapiro step, [25, 26] caused by a leaking high frequency noise. Indeed, Zn and Al samples have different V_0 values, requiring noise of very different frequency

within the same measurement apparatus. It also can't be attributed to a running state of an underdamped Josephson junction. [27] The underdamped regime would require a capacitance *four* orders of magnitude larger than that of our system. External capacitance is also excluded by the fact that the same results were obtained in two refrigerators with very different circuitry. Moreover, contrary to the observed plateau, voltage across an underdamped junction is expected to grow with the increased current bias.

Key to understanding these observations are non-equilibrium quasiparticles [18] generated by PSs. In our samples (in contrast with previous studies [13–16, 18]) the inelastic relaxation length L_{in} exceeds the wire length [17], allowing the quasiparticles to spread over the entire wire. At the interfaces with the leads the quasiparticles experience Andreev reflections, which mix particles and holes. This leads to quasiparticle diffusion over energy [28], resulting in a peculiar non-equilibrium distribution. Because of the self-consistency relation, such a non-equilibrium distribution suppresses the order parameter Δ inside the wire (relative to its equilibrium value Δ_0). Although the quasiparticles are far

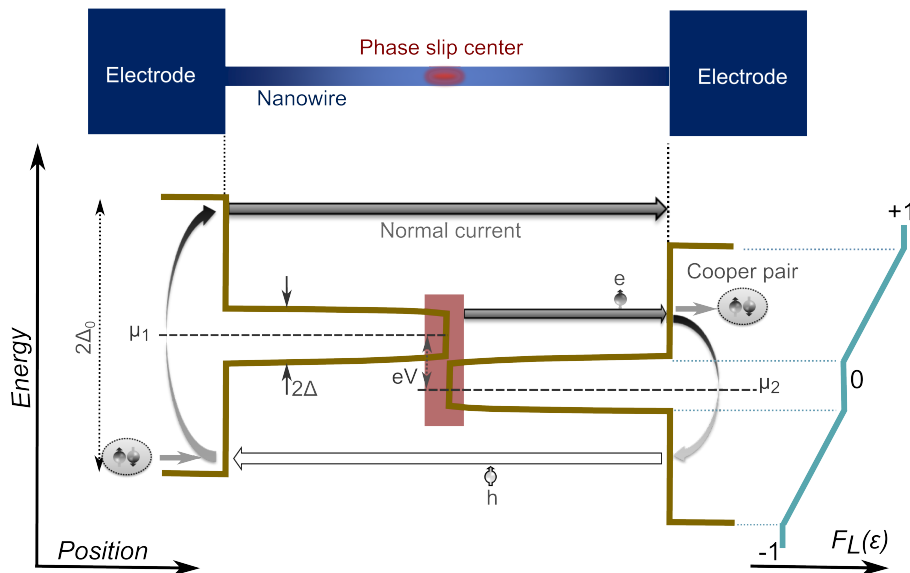


Figure 3. **Dissipative superconducting state of the nanowire.** (Top) Schematic of the system: superconducting nanowire is connected to superconducting leads. (Bottom) The energy gap profile as a function of position along the system. Phase slips occur in the center of the wire, generating non-equilibrium quasiparticles. At the two wire-lead interfaces, they experience multiple Andreev reflections before escaping into the leads. This establishes a universal distribution, with the longitudinal part $F_L(\epsilon)$ shown on the right. The self-consistency relation (2) results in the suppressed non-equilibrium gap $2\Delta \approx 0.34\Delta_0$, dictating that the voltage $eV_0 = 2\Delta$ should develop to maintain PSs events.

from equilibrium, the order parameter is fixed to its local self-consistent value everywhere apart from a distance $\sim \xi$ around the PS. The *condensate* chemical potential μ , given by the Josephson relation $\mu = \hbar\langle\partial_t\phi\rangle/2$, thus exhibits a discontinuity eV at the PS location[18]. Since the leads absorb high-energy quasiparticles, the concentration of the latter is largest in the center, pinning the PS to the midpoint of the wire. For PS's to occur, the voltage must exceed the energy gap, Fig. 3, i.e. $eV_0 \approx 2\Delta$. In this case PSs keep generating quasiparticles, self-propelling the dissipative state.

For a quantitative description [19] it is convenient to parametrize the quasiparticle distribution function $F(\epsilon, x) = 1 - 2n(\epsilon, x)$ by its longitudinal and transverse components, which are its odd and even parts $F_{L/T}(\epsilon, x) = F(\epsilon - \mu_a, x) \mp F(-\epsilon + \mu_a, x)$ with respect to the two chemical potentials $\mu_{1,2} = \pm eV/2$. At the boundaries with the leads $x = x_{1,2}(\epsilon)$ they obey Andreev boundary conditions:

$$F_T(\epsilon, x)|_{x=x_a(\epsilon)} = 0; \quad \partial_x F_L(\epsilon, x)|_{x=x_a(\epsilon)} = 0. \quad (1)$$

In the absence of inelastic relaxation the continuity relation (known also as the Usadel equation[29, 30]) reads $\partial_x F_{L/T}(\epsilon, x) = J_{L/T}(\epsilon)$, which along with Eq. (1) leads to x -independent $F_L(\epsilon)$ (for $|\epsilon| < \Delta_0$), satisfying the energy-diffusion equation[28] $\partial_\epsilon^2 F_L = 0$. Since the self-consistency relation

$$\int_{\Delta(x)}^{\omega_D} d\epsilon \frac{F_L(\epsilon, x)}{\sqrt{\epsilon^2 - \Delta^2(x)}} = \int_{\Delta_0}^{\omega_D} d\epsilon \frac{\tanh(\epsilon/2T)}{\sqrt{\epsilon^2 - \Delta_0^2}} \quad (2)$$

(ω_D is Debye frequency) involves only F_L , it results in an almost constant $\Delta(x) \approx \Delta$. The PSs in the middle of the wire excite quasiparticles and holes, equilibrating their populations. This provides the boundary condition $F_L(|\epsilon| < \Delta) = 0$ for the energy diffusion [28], resulting in the distribution function depicted in Fig. 3. Being substituted into the self-consistency relation (2), it results in a transcendental equation for $\delta = \Delta/\Delta_0$, which at $T = 0$ has two solutions (bistability!): $\delta_{sc} = 1$ and $\delta_{vp} = 0.17$.

The second of these solutions implies a *dissipative* state with $eV_0 = 2\Delta \approx 0.34\Delta_0$. It is sustained if a normal current $I_b \approx 1.64(V_0/R_n)$ [19], is applied to the wire. Notice that for $\xi \ll L$ the current I_b is much smaller than the departing critical current, allowing the wire to still support a supercurrent. An excess current $I - I_b$ is thus carried as the supercurrent without an additional voltage increase - hence the observed voltage plateau. The current exceeding $I_t \approx 0.72\Delta_0/eR_n$ stabilizes another solution of the self-consistency and the energy diffusion equations: the one with vanishing order parameter in the middle of the wire. It essentially terminates the supercurrent, resulting in the resistance being close to the normal one. The fact that these threshold values are about 30% less than the observed ones is attributed to the residual inelastic processes, neglected above. Indeed, the latter lead to particle-hole recombination, driving the distribution towards the equilibrium one. A reasonable estimate $L_{in} \approx 12\mu m$ [17] brings the currents $I_{b,t}$ as well as the voltage plateau V_0 within 10% of the observed values.

This picture also naturally accounts for the observed

effects of the magnetic field and temperature. The field mostly suppresses the order parameter of the *leads* Δ_{lead} , leaving that of the wire (almost) intact. This narrows the interval for the energy diffusion[31], bringing the distribution closer to the equilibrium one. This in turn increases the bottom threshold current I_b . For $\Delta_{lead} \lesssim 0.78\Delta_0$ the self-consistent solution of Fig. 3 with $\delta \neq 1$ is not possible anymore. The superconducting state of the wire is thus stabilized all the way up to I_t . In fact, suppression of Δ_{lead} is also the primary mechanism of the voltage plateau termination at $T \gtrsim 650$ mK, Fig. 1b.

-
- [1] P. de Gennes, *Superconductivity of Metals and Alloys* (Westview Press: 2nd edition, 1999).
- [2] G. Blatter, M. V. Feigel'man, V. B. Geshkenbein, A. I. Larkin, and V. M. Vinokur, *Vortices in high-temperature superconductors*, *Rev. Mod. Phys.* 66, 1125 (1994).
- [3] G. N. Gol'tsman, O. Okunev, G. Chulkova, A. Lipatov, A. Semenov, K. Smirnov, B. Voronov, A. Dzardanov, C. Williams, and R. Sobolewski, *Picosecond superconducting single-photon optical detector*, *Applied Physics Letters* 79, 705 (2001).
- [4] M. D. Eisaman, J. Fan, A. Migdall, and S. V. Polyakov, *Invited Review Article: Single-photon sources and detectors*, *Review of Scientific Instruments* 82, (2011).
- [5] J. Clarke and F. K. Wilhelm, *Superconducting quantum bits*, *Nature* 453, 1031 (2008).
- [6] M. H. Devoret and R. J. Schoelkopf, *Superconducting Circuits for Quantum Information: An Outlook*, *Science* 339, 1169 (2013).
- [7] D. A. Wollman, D. J. Van Harlingen, W. C. Lee, D. M. Ginsberg, and A. J. Leggett, *Experimental determination of the superconducting pairing state in YBCO from the phase coherence of YBCO-Pb dc SQUIDS*, *Phys. Rev. Lett.* 71, 2134 (1993).
- [8] C. C. Tsuei, J. R. Kirtley, C. C. Chi, L. S. Yu-Jahnes, A. Gupta, T. Shaw, J. Z. Sun, and M. B. Ketchen, *Pairing Symmetry and Flux Quantization in a Tricrystal Superconducting Ring of YBa₂Cu₃O_{7- δ}* , *Phys. Rev. Lett.* 73, 593 (1994).
- [9] J. E. Mooij and Y. V. Nazarov, *Superconducting nanowires as quantum phase-slip junctions*, *Nat Phys* 2, 169 (2006).
- [10] A. Bezryadin, *Superconductivity in Nanowires: Fabrication and Quantum Transport* (Wiley-VCH: 1 edition, 2012).
- [11] F. Altomare and A. M. Chang, *One-Dimensional Superconductivity in Nanowires* (Wiley-VCH: 1st edition, 2013).
- [12] K. Yu Arutyunov, D. S. Golubev, and A. Zaikin, *Superconductivity in one dimension*, *Physics Reports* 464, 1 (2008).
- [13] M. Sahu, M.-H. Bae, A. Rogachev, D. Pekker, T.-C. Wei, N. Shah, P. M. Goldbart, and A. Bezryadin, *Individual topological tunnelling events of a quantum field probed through their macroscopic consequences*, *Nat Phys* 5, 503 (2009).
- [14] N. Shah, D. Pekker, and P. M. Goldbart, *Inherent Stochasticity of Superconductor-Resistor Switching Behavior in Nanowires*, *Phys. Rev. Lett.* 101, 207001 (2008).
- [15] P. Li, P. M. Wu, Y. Bomze, I. V. Borzenets, G. Finkelstein, and A. M. Chang, *Switching Currents Limited by Single Phase Slips in One-Dimensional Superconducting Al Nanowires*, *Phys. Rev. Lett.* 107, 137004 (2011).
- [16] M. Singh and M. H. W. Chan, *Observation of individual macroscopic quantum tunneling events in superconducting nanowires*, *Phys. Rev. B* 88, 064511 (2013).
- [17] M. Stuivinga, J. E. Mooij, and T. M. Klapwijk, *Current-induced relaxation of charge imbalance in superconducting phase-slip centers*, *Journal of Low Temperature Physics* 46, 555 (1982).
- [18] W. Skocpol, M. R. Beasley, and M. Tinkham, *Phase-slip centers and nonequilibrium processes in superconducting tin microbridges*, *Journal of Low Temperature Physics* 16, 145 (1974).
- [19] see Supplementary Materials.
- [20] Y. Chen, S. D. Snyder, and A. M. Goldman, *Magnetic-Field-Induced Superconducting State in Zn Nanowires Driven in the Normal State by an Electric Current*, *Phys. Rev. Lett.* 103, 127002 (2009).
- [21] Y. Chen, Y.-H. Lin, S. D. Snyder, and A. M. Goldman, *Stabilization of superconductivity by magnetic field in out-of-equilibrium nanowires*, *Phys. Rev. B* 83, 054505 (2011).
- [22] M. Tian, N. Kumar, S. Xu, J. Wang, J. S. Kurtz, and M. H. W. Chan, *Suppression of Superconductivity in Zinc Nanowires by Bulk Superconductors*, *Phys. Rev. Lett.* 95, 076802 (2005).
- [23] M. Tian, N. Kumar, J. Wang, S. Xu, and M. H. W. Chan, *Influence of a bulk superconducting environment on the superconductivity of one-dimensional zinc nanowires*, *Phys. Rev. B* 74, 014515 (2006).
- [24] R. Tidecks, *Current-Induced Nonequilibrium Phenomena in Quasi-One-Dimensional Superconductors* (Springer: 1 edition, 1990).
- [25] R. C. , M.-H. Bae, and A. Bezryadin, *Applied Physics Letters* 93, (2008).
- [26] M.-H. Bae, R. C. Dinsmore III, M. Sahu, and A. Bezryadin, *Stochastic and deterministic phase slippage in quasi-one-dimensional superconducting nanowires exposed to microwaves*, *New Journal of Physics* 14, 043014 (2012).
- [27] A. Barone and G. Paterno, *Physics and Applications of the Josephson Effect* (Wiley-VCH: 1 edition, 1982).
- [28] K. E. Nagaev, *Frequency-Dependent Shot Noise in Long Disordered Superconductor/Normal-Metal/Superconductor Contacts*, *Phys. Rev. Lett.* 86, 3112 (2001).
- [29] K. D. Usadel, *Generalized Diffusion Equation for Superconducting Alloys*, *Phys. Rev. Lett.* 25, 507 (1970).
- [30] A. Kamenev, *Field Theory of Non-Equilibrium Systems* (Cambridge University Press, 2011).
- [31] D. Y. Vodolazov and F. M. Peeters, *Enhancement of the retrapping current of superconducting microbridges of finite length*, *Phys. Rev. B* 85, 024508 (2012).

METHODS

Investigated Zn nanowires are 100–120 nm wide, 65–110 nm high, with the length $1.5\mu\text{m} < L < 6\mu\text{m}$ (see Table I in Supplemental material) connected to four $1\mu\text{m}$ wide

Zn electrodes, inset to Fig. 1a. The Zn electrodes are 10 μm long and in turn are connected to pre-patterned Au contacts. Both the nanowire and the electrodes were fabricated in a single step of the quench-deposition at 77K substrate temperatures, depositing through a resist mask patterned using electron-beam lithography. The normal state resistivity varies $\rho = (6.2 - 8.4) * 10^{-8} \Omega\text{m}$, in comparison the bulk value for Zn is $\rho = 5.9 * 10^{-8} \Omega\text{m}$.

The electrical measurements were carried out in two different refrigerators: (1) Oxford Kelvinox-400 dilution refrigerator, with the minimum temperature of 50 mK. The associated electrical lines were heavily filtered with RC filters at room temperature with a cutoff frequency around 100Hz and with thermo coaxial cable filters at low temperature with a cutoff frequency around 1 GHz. (2) Quantum Design Physical Properties Measurement System equipped with a He-3 insert, with no filtering system other than having the electrical lines twisted in pairs.

To bypass effects of noise, the time domain data was taken only in the refrigerator 1. The electrical measurements were performed with a bandwidth of 12 Hz and a repetition rate of 3 Hz. At a fixed current in the transition regime, voltage was continuously measured for 1800 seconds, exhibiting random switching in real time. To extract characteristic lifetimes of the superconducting τ_{sc} and the voltage plateau τ_{vp} states the first 100-seconds of data was discarded, in order to bypass possible transients. After that, whenever the voltage crossed above or

below a threshold value (defined as 3 times the noise floor of the measurement setup: ~ 80 nV), the switching into or out of the voltage plateau state was recorded. The time intervals between two consecutive switching events defined residence times in one state. Finally, τ_{sc} and τ_{vp} , reported in the main text, are mean values of the stochastic residence time sequence, collected over 1800 seconds.

ACKNOWLEDGMENTS

Experimental work at Minnesota was supported by the DOE Office of Basic Energy Sciences under Grant No. DE-FG02-02ER4600. Samples were fabricated in the Nano Fabrication Center, which receives funding from the NSF as a part of the NNIN, and were characterized in the Characterization Facility, University of Minnesota, a member of the NSF-funded Materials Research Facilities Network (<http://www.mrfn.org>) via the MR-SEC program. AK was supported by DOE Contract No. DE-FG02-08ER46482.

CONTRIBUTIONS

All the authors contribute exclusively to this work.

COMPETING FINANCIAL INTERESTS

The authors declare no competing financial interests.

Sample	Material	Growth Parameters			Measured Parameters			
		Length (μm)	Height (nm)	Width (nm)	T_c (K)	R_n (Ω)	V_0 (V)	V_0/Δ_0
A	Zn	4.5	65	100	0.76	52	52.5	0.46
B	Zn	4.0	60	100	0.77	41	41.0	0.35
C	Zn	4.5	65	110	0.75	53	44.7	0.40
D	Al	3.0	50	50	1.25	23	93.2	0.49

Table I. List of parameters for all studied samples. Critical temperature T_c is taken as the temperature of the half-normal resistance at a low applied current of $0.1 \mu\text{A}$; the BCS energy gap is defined as $2\Delta_0 = 3.52T_c$. Plateau voltage V_0 is the averaged voltage over the entire plateau regime.

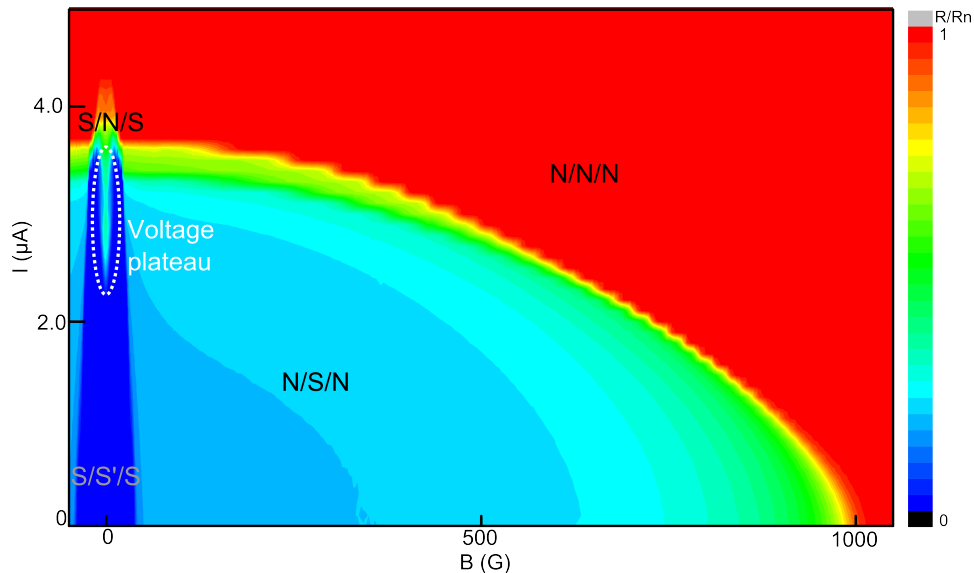


Figure 1. Resistance color map of sample B, along the axes of magnetic field and current. Regimes are labeled according to the states of the lead/nanowire/lead system. The highlighted area is the voltage plateau regime discussed in the main text.

I. SUPPLEMENTAL EXPERIMENTAL DATA

Figure 1 shows the resistance false-colored map for sample B at 450 mK, as a function of perpendicular magnetic field and applied current. It complements the phase diagram of Fig. 2e of the main text, showing a broader range of the perpendicular magnetic fields. One may distinguish between different regimes of the total system, as denoted in the figure:

1) N/N/N regime (red-colored): at high fields and high currents, both the nanowire and the leads are driven into the normal state. As a consequence, the system retains its full normal resistance. 2) S/S'/S regime (blue-colored): at low currents and low fields, both the nanowire and the leads are superconducting. 3) N/S/N regime (light blue-colored): at a critical field ~ 40 G the leads turn normal; the narrow wire expels the field and thus remains superconducting until much larger fields. The system exhibits a small non-zero resistance. We believe, it is primarily coming from the parts of the wire of length $\sim \xi$ which are in direct proximity to the normal leads. As the field increases it weakens the superconductivity in the wire, increasing its coherence length and thus the proximity-induced resistance. The entire wire turns into the normal state at ~ 1000 G. 4) S/N/S regime (light green-colored near zero field): at low field and high currents, the system is in the regime, where the leads are superconducting while the nanowire is driven into normal state by the applied current. This is the regime that is described as the “proximitized normal” in the main text. The nanowire is almost entirely normal save for a slightly reduced resistance, due to the proximity with the superconducting leads. 5) The *voltage plateau regime* (encircled by white dotted line) takes place at low fields and intermediate currents. Distinct from S/N/S regime, the voltage plateau regime is seen to be embedded into the S/S'/S regime. This suggests that, despite presence of a finite voltage V_0 and thus the dissipation, the superconducting order in the nanowire is not entirely suppressed.

Extensive measurements at the onset of the voltage plateau were performed by sustaining a fixed current for 1800 seconds and repeatedly measuring voltage with a repetition rate of 3 Hz. Total of 5400 measurements were collected and the distribution function of measured voltages was constructed. Figure 2(a) shows such distribution functions plotted for different currents across the transition regime for sample A at 50 mK. The graph exhibits two distinct peaks: one centered at zero voltage and the other centered at the voltage plateau. This provides evidence to a bistable nature of the system across the transition regime, meaning it has non-zero probabilities of occupying the superconducting state and the voltage plateau states. Though the mechanism that drives this switching remains unknown. Some important insights may be obtained from measurements at different temperatures. Shown in Fig. 2(b), is the temperature dependence of τ_{vp} and τ_{sc} , defined in the main text, at the current of $1.95 \mu A$. One can clearly see that neither τ_{vp} nor τ_{sc} is significantly modified by the increasing temperature up to about ~ 400 mK. At even higher temperature stability of the

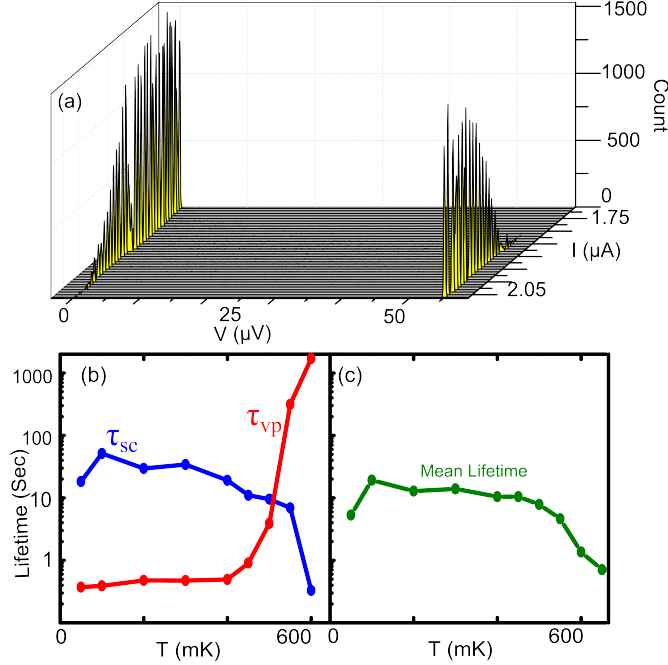


Figure 2. a) Voltage distributions for various currents in the transition region. For each current the distribution is extracted from 5400 single-shot measurements at zero magnetic field, at 50 mK. b) τ_{sc} and τ_{vp} as functions of temperature for current $1.95 \mu\text{A}$. c) The mean lifetime of the system, defined as the mean switching time at the current where $\tau_{sc} = \tau_{vp}$, as a function of temperature.

dissipative state rapidly increases, while that of the superconducting state – decreases. To further quantify the temperature dependence of the switching rates we plot, Fig. 2(c), mean lifetime of the system at a current when $\tau_{vp} = \tau_{sc}$. Similarly to the behavior of τ_{vp} and τ_{sc} , increasing the temperature has a negligible impact on the system below ~ 400 mK. Above it, increasing temperature leads to the reduction of the mean lifetime, indicating the switchings occur more frequently at higher temperatures.

II. SUPPLEMENTAL THEORETICAL DISCUSSION

We assume that the order parameter $\Delta(x)$ coincides locally with the spectral gap, while the local density of states is given by $\nu\epsilon/\sqrt{\epsilon^2 - \Delta^2(x)}$. Strictly speaking, this is not the case in the presence of a supercurrent and/or an external magnetic field. In these cases the peak in the density of states is rounded and the spectral gap is somewhat smaller than Δ . However since all relevant currents and fields are much less than the corresponding depairing values,

one may safely neglect this difference. For the time being we shall also disregard the inelastic relaxation processes, having in mind that the nanowires are shorter than the inelastic length. Under these assumptions the Usadel equation [1, 2] for the distribution function takes the form of the continuity equation for the two components of the distribution function $F(\epsilon, x, t)$, defined in the main text

$$\partial_t F_{L/T} + \partial_x [D_{L/T} \partial_x F_{L/T}] = 0, \quad (1)$$

where $D_L = D$ and $D_T(\epsilon, x) = D\epsilon^2/(\epsilon^2 - \Delta^2(x))$ and D is the normal-state diffusion constant.

Let $x_{1,2}(\epsilon)$ be the points of Andreev reflections for quasiparticles with energy ϵ from left/right leads, i.e. $\Delta(x_{1,2}) = \epsilon$. Due to the x -reflection plus particle-hole symmetries, $x \rightarrow -x$ and $\epsilon \rightarrow -\epsilon$, of the system $x_{1,2}(\epsilon) = \mp x(\epsilon \mp V/2)$. The stationary solution of the Usadel equation (1) takes the form

$$F(\epsilon, x) = F_L(\epsilon) + J_T(\epsilon)x, \quad (2)$$

where due to particle-hole symmetry, $F_L(\epsilon) = -F_L(-\epsilon)$ and $J_T(\epsilon) = J_T(-\epsilon)$. At the two Andreev interfaces the distribution function obeys the following boundary conditions:

$$F(\epsilon, x_{1,2}) = -F(-\epsilon \pm V, x_{1,2}); \quad \partial_x F(\epsilon, x_{1,2}) = \partial_x F(-\epsilon \pm V, x_{1,2}). \quad (3)$$

Substituting Eq. (2), shifting the energy by $V/2$ and employing the symmetry properties, one finds

$$F_L(\epsilon + V/2) - J_T(\epsilon + V/2)x(\epsilon) = F_L(\epsilon - V/2) + J_T(\epsilon - V/2)x(\epsilon)$$

and

$$J_T(\epsilon + V/2) = J_T(\epsilon - V/2).$$

In the leading order in voltage one finds $J_T(\epsilon) = J_T = \text{const}$, where

$$J_T = \frac{V}{2x(\epsilon)} \partial_\epsilon F_L(\epsilon).$$

Bringing back slow time dependence and weak inelastic relaxation, one may rewrite these results [3] as the diffusive equation in the energy direction for the longitudinal (antisymmetric) component

$$\partial_t F_L(\epsilon, t) = \partial_\epsilon \left(\mathcal{D}(\epsilon) \partial_\epsilon F_L(\epsilon, t) \right) + I_{in}[F_L], \quad (4)$$

where the energy diffusion coefficient is given by [3]

$$\mathcal{D}(\epsilon) = \frac{DV^2}{L^2(\epsilon)}; \quad (5)$$

here $L(\epsilon) = 2x(\epsilon)$ is the length between the two Andreev boundaries for quasiparticles at energy ϵ . The inelastic collision term I_{in} in the simplest relaxation time approximation takes the form

$$I_{in}[F_L] = \frac{1}{\tau_{in}} \left(\tanh \frac{\epsilon}{2T} - F_L(\epsilon, t) \right).$$

Although these equations were rigorously derived only in the limit of small voltage, they remain at least semi-quantitatively valid all the way up to $V \approx \Delta_0$.

Let us assume first that the order parameter is completely suppressed in the middle of the wire. This is the case at the *top* threshold current I_t . In the absence of the inelastic relaxation the corresponding stationary solution of Eq. (4) at $T = 0$ takes the form $F_L(\epsilon) = \epsilon/\tilde{\Delta}$ for $|\epsilon| < \tilde{\Delta}$ and $F_L(\epsilon) = \text{sign}(\epsilon)$ for $|\epsilon| > \tilde{\Delta}$. Here $\tilde{\Delta} = \Delta_0 + V_t/2$ is the energy window, where multiple Andreev scattering take place and we put $L(\epsilon) = L$. Substituting it into the self-consistency relation (2) of the main text with $\Delta(x) = 0$, one obtains $\ln(2\tilde{\Delta}/\Delta_0) = 1$, which results in $V_t = (e - 2)\Delta_0 \approx 0.72\Delta_0$.

Inelastic relaxation cools down the quasiparticles, leading to a somewhat larger V_t . Indeed, assuming for simplicity energy independent τ_{in} , one finds for the stationary solution of Eq. (4) for e.g. $\epsilon > 0$

$$F_L(\epsilon) = \frac{e^{2\tilde{\Delta}/\epsilon_{in}}(1 - e^{-\epsilon/\epsilon_{in}}) - (1 - e^{\epsilon/\epsilon_{in}})}{e^{2\tilde{\Delta}/\epsilon_{in}} - 1},$$

where $\epsilon_{in} = \sqrt{V^2 D/L^2 \tau_{in}} = V L_{in}/L$. Substituting into the self-consistency relation, one finds to the leading order in $\tilde{\Delta}/\epsilon_{in} < 1$: $\ln(2\tilde{\Delta}/\Delta_0) = 1 + \tilde{\Delta}^2/12\epsilon_{in}^2$. This may be satisfied only if $\epsilon_{in} > 0.9\Delta_0$, while for a faster inelastic relaxation the multiple Andreev reflections can't suppress the superconductivity. For a slower inelastic relaxation the top voltage (the one the system acquires at a current slightly larger than the top threshold current, i.e. $I \gtrsim I_t$) is found to be $V_t \approx \Delta_0(0.72 + 0.81(L/L_{in})^2)$.

We turn now to the bottom critical current I_b . In this case the order parameter is only partially suppressed down to $0 < \Delta < \Delta_0$ inside the wire. This requires the voltage $V_0 \approx 2\Delta$ to cut through the order parameter and allow for PSs. In other words: frequency of PS's is given by $2V$, while duration of a single PS is about 4Δ [4]; for the order parameter to be continuously suppressed at PS location the voltage should be at least 2Δ . The continuous train of PSs equilibrates quasiparticles and holes immediately below and above the suppressed gap, leading to the boundary condition $F_L(|\epsilon| < \Delta) = 0$. The corresponding solution of

Eq. (4) with no inelastic relaxation takes the form

$$F_L(\epsilon) = \begin{cases} 0 & 0 < \epsilon < \Delta; \\ (\epsilon - \Delta)/(\Delta_{lead} - \Delta) & \Delta < \epsilon < \Delta_{lead}; \\ 1 & \Delta_{lead} < \epsilon. \end{cases} \quad (6)$$

It is depicted in Fig. 3 of the main text for the case $\Delta_{lead} = \Delta_0$, i.e. at $T = 0$ and in the absence of magnetic field. Substituting this distribution function into the self-consistency relation, one finds a closed transcendental equation for $\delta = \Delta/\Delta_{lead}$:

$$\sqrt{1 - \delta^2} - \ln\left(1 + \sqrt{1 - \delta^2}\right) + (1 - \delta) \ln(\Delta_0/\Delta_{lead}) = \delta \ln(1/\delta). \quad (7)$$

For $\Delta_{lead} = \Delta_0$ it admits two solutions: $\delta = 1$ – the superconducting state with no PSs and $\delta = 0.17$ – the dissipative state with the PSs train. Therefore in the presence of phase slips and in the absence of inelastic relaxation the wire sustains the (nearly space-independent) suppressed order parameter $\Delta \approx 0.17\Delta_0$. As before, the inelastic relaxation cools down the quasiparticles and thus increases the suppressed self-consistent order parameter of the wire. The calculation analogous to the one outlined above leads to $\Delta \approx \Delta_0(0.17 + 0.53(L/L_{in})^2)$. As a result the corresponding voltage plateau acquires the value $V_0 \approx \Delta_0(0.34 + 1.06(L/L_{in})^2)$.

Voltage causes a normal current $I_n = \nu \int d\epsilon D_T(\epsilon) J_T(\epsilon)$ to flow across the wire. For not too large voltage $V \lesssim 2\Delta_0$ one finds $J_T(\epsilon) = \partial_\epsilon F_L(\epsilon) eV/L$. The energy integration over the range $|\epsilon| < \Delta_0 + V/2$ yields the logarithmically divergent integral, which is to be cut at $|\epsilon - \Delta| \approx V$. As a result, for $V = V_0$ one obtains $I_n = (1 + 2\delta - \delta \ln \delta) V_0/R_n$, where $R_n = L/(e^2 \nu D)$ is the normal state resistance of the wire. We thus find that for the dissipative state to occur a minimal current $I_b \approx 1.64(V_0/R_n)$ should be supplied to pass through the wire. Since the order parameter is totally suppressed only in PS region of size $\sim \xi$, the wire may still support the supercurrent I_{sc} in addition to the normal one. While the latter is carried by quasiparticles undergoing multiple Andreev reflections, the former is due to the small phase gradient of the (suppressed) order parameter $\Delta(x) = \Delta e^{i\phi x/L}$. As a result the current in excess of I_b is carried as the supercurrent, exhibiting the voltage plateau pattern. However once the total current reaches I_t , the system becomes unstable against transition to the state with zero order parameter across the wire, discussed above. This eliminates the supercurrent and thus for $I > I_t$ the wire's resistance is close to R_n .

The main effect of the magnetic field or elevated temperature is to suppress the equilibrium order parameter inside the leads $\Delta_{lead} < \Delta_0$. This narrows the energy window for the Andreev diffusion, Eq. (4). Numerical investigation of transcendental equation (7) shows that the non-trivial solution is only possible as long as $\Delta_{lead} \geq 0.78\Delta_0$, otherwise the dissipative state with a non-zero order parameter is not sustainable. The quantitative comparison in case of the perpendicular magnetic field requires knowledge of the leads order parameter next to the contact with the wire. This would demand knowing precise location of the vortices in the leads. On the other hand, the temperature dependence is rather straightforward. Taking as an example sample A with the critical temperature $T_c = 0.76$ K and using standard BCS expressions one estimates that the order parameter is suppressed by the factor 0.78 relative to its $T = 0$ value at $T \approx 0.75T_c \approx 0.59$ K. This is in a reasonable agreement with $T = 0.65$ K observed as the upper temperature limit of the voltage plateau, Fig 1b of the main text. The difference may be again attributed to the residual inelastic processes, which cool down the non-equilibrium distribution.

-
- [1] K. D. Usadel, Generalized Diffusion Equation for Superconducting Alloys, Phys. Rev. Lett. 25, 507 (1970).
 - [2] A. Kamenev, Field Theory of Non-Equilibrium Systems (Cambridge University Press, 2011).
 - [3] K. E. Nagaev, Frequency-Dependent Shot Noise in Long Disordered Superconductor\Normal-Metal\Superconductor Contacts, Phys. Rev. Lett. 86, 3112 (2001).
 - [4] K. Yu Arutyunov, D. S. Golubev, and A. Zaikin, Superconductivity in one dimension, Physics Reports 464, 1 (2008).